Waveguide Discontinuity Analysis with a Coupled Finite–Boundary Element Method

KE LI WU, GILLES Y. DELISLE, SENIOR MEMBER, IEEE, DA GANG FANG, AND MICHEL LECOURS, SENIOR MEMBER, IEEE

Abstract—A new numerical method for the analysis of waveguide discontinuities is proposed. The proposed approach is based upon the coupling of the finite element and boundary element methods. The respective merits of these methods are extracted to yield much faster solution and to enhance computation efficiency. A general procedure is described using a quadratic elements approximation, and the validity and efficiency of the method are demonstrated in the cases of a 3-port H-plane ferrite waveguide Y junction and of a right-angle corner bend with and without dielectric loading. Comparisons of the present results with those obtained using the finite element approach are made and shown to be in good agreement. An experimental result is also presented and the validity of the technique can be easily verified.

I. Introduction

MANY NUMERICAL and analytical methods are now available to solve the problem of waveguide discontinuities, a situation which arises very often in the design of microwave components or circuits. Some of the numerical methods apply only to specific waveguide boundaries [1], [2] due to the choice of the Green's function, and some are restricted to the analysis of particular shapes of junctions and obstacles inside the waveguide [3], [4]. Numerical methods which can solve arbitrary waveguide configurations are also available and one of these approaches is based on the finite element method (FEM) [5]–[7], which is a very powerful technique that can handle discontinuities of arbitrary shape, including anisotropic waveguide components such as ferrite junction circulators. However, this method requires very large computer memory space and considerable computation time to yield a valid solution to the final matrix equation. More recently, the application of the boundary element method (BEM) [8] to waveguide discontinuity problems has been proposed [9], [10]. Because the BEM calls for a solution which makes it possible to decrease by one the dimension of the original problem, it requires much less computer memory and the computation time is also reduced appreciably. Nevertheless, it is quite difficult to treat a problem involving complex or anisotropic media with the BEM.

In this paper, the FEM and BEM techniques are coupled together to obtain a new method, called the coupled finite–boundary element method (CFBM), which has the merits of both the FEM and the BEM and can solve extremely complex problems without requiring excessive computer memory and computation time. Using this method, only the complex media subdomains which could be constituted by lossy or anisotropic materials need to be treated with the finite element approach. Elsewhere, the boundary element method is used on the boundary to take into account the waveguide configuration.

The application of the CFBM to a particular problem is quite straightforward. First, each complex subdomain is approximated using finite elements, and the field in each element is expressed using an interpolation technique. The Galerkin procedure is then used to obtain the relation between the fields on the complex media subdomain and the normal derivatives of the fields on its boundary. Subsequently the BEM is used to obtain the boundary integral equation on the complementary homogeneous domain which leads to a system equation. With the help of the analytical expression of the fields and of their normal derivatives on the ports, the two system equations are combined using the continuity on the interface of two different subdomains, and a final matrix equation is obtained.

The validity of the CFBM will be demonstrated with illustrative examples. The results obtained with the proposed CFBM and those obtained by FEM alone are compared and shown to be in good agreement. In the present CFBM analysis, the power conservation condition is satisfied to an accuracy of $\pm 10^{-5}$ to 10^{-4}.

II. Analytical Formulation

In order to minimize the details, only the H-plane waveguide discontinuity problem shown in Fig. 1 will be addressed. If an M-port device is assumed, the boundary Γ_Q encloses the inhomogeneous subdomain and the boundary $\Gamma' = B \cup \Gamma$, where $\Gamma = \bigcup_{m=0}^{M} \Gamma_m$, completely encloses the remaining homogeneous domain (Fig. 2).

Manuscript received March 21, 1988; revised December 16, 1988.

K. L. Wu, G. Y. Delisle, and M. Lecours are with the Electrical Engineering Department, Laval University, Quebec City, Canada G1K 7P4.

D. G. Fang is with the Electrical Engineering Department, East China Institute of Technology, Nanjing, China.

IEEE Log Number 8927156.

0018-9480/89/0600-0993$01.00

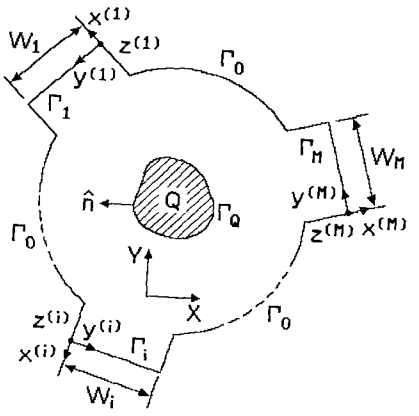

Fig. 1. Geometry of the problem and FEM region Q.

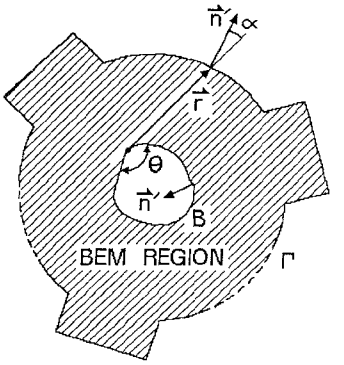

Fig. 2. BEM complex homogeneous region surrounded by Γ and B.

A. FEM Formulation

Using the technique introduced here, complex subdomains such as dielectric or ferrite posts can be treated with the FEM. With the finite element approach, the primary dependent variables are replaced by a system of discrete variables over the domain under consideration. Therefore, the subdomain itself is discretized into finite elements. The compatibility within the element and between element boundaries is ensured by the choice of the shape function. For this analysis, second-order triangular elements are used. That is, within each element, the electric field E_z is expressed in terms of the electric field at the corner and midside nodal points by

$$E_z = \{N\}^T \{E_z\}_e \tag{1}$$

where $\{E_z\}_e$ is the electric field vector corresponding to the nodal points within each element and $\{N\}$ is the shape function vector.

Considering the excitation to be the dominant TE_{10} mode and enforcing the continuity of the tangential magnetic field, the solution for the field inside the subdomain Q (see Fig. 1) is obtained from Maxwell's equations, using the Galerkin procedure and integration by parts; the results can be expressed as

$$[A]\{E_z\} - \sum_e{}' \int_e \{N\} \frac{\partial E_z}{\partial n}\bigg|_{\Gamma_Q} d\Gamma = \{0\} \tag{2}$$

$$[A] = \sum_e \iint \left[\frac{\mu_0}{\mu^2 - \kappa^2} \left\{ \mu \left(\frac{\partial\{N\}}{\partial x} \frac{\partial\{N\}^T}{\partial x} + \frac{\partial\{N\}}{\partial y} \frac{\partial\{N\}^T}{\partial y} \right) + j\kappa \left(\frac{\partial\{N\}}{\partial x} \frac{\partial\{N\}^T}{\partial y} - \frac{\partial\{N\}}{\partial y} \frac{\partial\{N\}^T}{\partial x} \right) \right\} - \epsilon_r (1 - j\tan\delta) k_0^2 \{N\}\{N\}^T \right] dx\,dy \tag{3}$$

where

$$k_0^2 = \omega^2 \epsilon_0 \mu_0 \tag{4}$$

and the permeability tensor $[\mu]$,

$$[\mu] = \begin{bmatrix} \mu & -j\kappa & 0 \\ j\kappa & \mu & 0 \\ 0 & 0 & \mu_0 \end{bmatrix} \tag{5}$$

is used [5]. Here, the components of the $\{E_z\}$ vector are the values of the electric field E_z at all nodal points in the subdomain Q; Σ_e and Σ_e' extend respectively over all different elements and the elements related to the boundary of Γ_Q. Equation (2) may be written as

$$\begin{bmatrix} [A]_{Q,\Gamma_Q} & [A]_{Q,Q} \\ [A]_{\Gamma_Q,\Gamma_Q} & [A]_{\Gamma_Q,Q} \end{bmatrix} \begin{Bmatrix} \{E_z\}_{\Gamma_Q} \\ \{E_z\}_Q \end{Bmatrix} = \begin{Bmatrix} \{0\} \\ [D]\left\{\frac{\partial E_z}{\partial n}\right\}_{\Gamma_Q} \end{Bmatrix} \tag{6}$$

where $\{E_z\}_Q$ and $\{E_z\}_{\Gamma_Q}$ are, respectively, the vectors of the electric field E_z at the nodal points inside Q and on the boundary of Q; $\{\partial E_z/\partial n\}_{\Gamma_Q}$ is the vector of the outward normal derivatives of E_z at the nodal points on the boundary of Q; $[A]_{Q,Q}$, $[A]_{Q,\Gamma_Q}$, $[A]_{\Gamma_Q,Q}$, and $[A]_{\Gamma_Q,\Gamma_Q}$ are the submatrices of $[A]$; and $[D]$ is a square coefficient matrix obtained through the integration of the shape function vector over the boundary Γ_Q.

B. BEM Formulation

Consider the remaining region surrounded by Γ_0, $\Gamma_1, \cdots, \Gamma_M$ and B, as shown in Fig. 2. Using the fundamental solution ϕ^* [8] and Green's formula, along with Maxwell's equations, the following equation for the field E_z^p can be obtained:

$$E_z^p + \int_{\Gamma'} \psi^* E_z \, d\Gamma = \int_{\Gamma'} \phi^* \frac{\partial E_z}{\partial n'} \, d\Gamma \tag{7}$$

where

$$\phi^* = \frac{1}{4j} H_0^{(2)}(k_0 r) \tag{8}$$

$$\psi^* = \frac{\partial \phi^*}{\partial n'} = \frac{j}{4} k_0 H_1^{(2)}(k_0 r) \cos\alpha. \tag{9}$$

Here, E_z^p is the electric field at the field point p; $H_0^{(2)}(\cdot)$ and $H_1^{(2)}(\cdot)$ are the zeroth- and first-order Hankel functions of the second kind, respectively; and α is the angle

between the vector $\vec{r}$ and the outward unit normal vector $\vec{n}$.

An approximate solution of (7) can be obtained by discretizing the contour into boundary elements. These boundary elements are similar to finite elements except that the dimension is one less than the dimension of the original problem. For the present analysis, second-order boundary elements are used for the sake of compatibility with the second-order finite elements.

Placing the field point $\vec{r}$ on the boundary Γ' and extracting the contribution of the singularity, the following equation can be obtained [10]:

$$\left(1-\frac{\theta}{2\pi}\right)E_z^p+\sum_e{}'[h_1,h_2,h_3]_e\begin{Bmatrix}E_z^1\\E_z^2\\E_z^3\end{Bmatrix}_e$$

$$=\sum_e{}'[g_1,g_2,g_3]_e\begin{Bmatrix}\dfrac{\partial E_z^1}{\partial n'}\\[2mm]\dfrac{\partial E_z^2}{\partial n'}\\[2mm]\dfrac{\partial E_z^3}{\partial n'}\end{Bmatrix}_e \tag{10}$$

where θ is the angle between boundary elements as specified in Fig. 2, and $\sum_e'$ extends over all elements on the boundary Γ'. Using matrix notation, (10) can be written more simply as

$$[[H]_0,[H]_1,\cdots,[H]_M,[H]_B]\begin{Bmatrix}\{E_z\}_{\Gamma_0}\\\{E_z\}_{\Gamma_1}\\\vdots\\\{E_z\}_{\Gamma_M}\\\{E_z\}_B\end{Bmatrix}$$

$$=[G]\begin{Bmatrix}\left\{\dfrac{\partial E_z}{\partial n'}\right\}_{\Gamma_0}\\\left\{\dfrac{\partial E_z}{\partial n'}\right\}_{\Gamma_1}\\\vdots\\\left\{\dfrac{\partial E_z}{\partial n'}\right\}_{\Gamma_M}\\\left\{\dfrac{\partial E_z}{\partial n'}\right\}_B\end{Bmatrix}. \tag{11}$$

This BEM matrix equation will be used later.

C. Analytical Approach

Assuming that the dominant TE_{10} mode is incident from port j, the analytical relation of the field and of its normal derivative at the ports is found as [10]

$$E_z(x^{(i)}=0,y^{(i)})=2\delta_{ij}\cdot f_{i1}(y^{(i)})-\sum_{m=1}^{\infty}\frac{1}{j\beta_{im}}\int_0^{W_i}f_{im}(y_0^{(i)})f_{im}(y^{(i)})\cdot\frac{\partial E_z}{\partial n'}(x^{(i)}=0,y_0^{(i)})\,dy_0^{(i)} \tag{12}$$

where

$$f_{im}(y^{(i)})=\sqrt{\frac{2}{W_i}}\sin(m\pi y^{(i)}/W_i),\qquad m=1,2,3,\cdots \tag{13}$$

$$\beta_{im}=\sqrt{k_0^2-(m\pi/W_i)^2},\qquad m=1,2,3,\cdots. \tag{14}$$

The discretized form of (12) by boundary elements leads to

$$\{E_z\}_{\Gamma_i}=2\delta_{ij}\{f_{i1}\}+[Z]_i\left\{\frac{\partial E_z}{\partial n'}\right\}_{\Gamma_i} \tag{15}$$

where

$$[Z]_i=-\sum_{m=1}^{\infty}(1/j\beta_{im})\{f_{im}\}\sum_{e'}\int_{e'}f_{im}(y_0^{(i)})\cdot\left\{N(x^{(i)}=0,y_0^{(i)})\right\}dy_0^{(i)},\qquad i=1,2,\cdots,M. \tag{16}$$

Here, the components of the $\{f_{im}\}$ vector are the values of $f_{im}(y^{(i)})$ at the nodal points on Γ_i, and $\Sigma_{e'}$ extends over the elements related to Γ_i.

D. Combination of FEM and BEM

In order to reduce the computational effort, it is better to enclose the inhomogeneous complex subdomain by an actual or an artificial boundary as small as possible, apply the FEM to the inhomogeneous subdomain, and use the BEM in the remaining homogeneous domain taking into account the waveguide configuration information.

On the complex domain boundary Γ', the following boundary conditions are taken:

$$\{E_z\}_{\Gamma_0}=\{0\}\qquad\text{on}\quad\Gamma_0 \tag{17}$$

$$\{E_z\}_{\Gamma_Q}=\{E_z\}_B\qquad\text{on}\quad\Gamma_Q \tag{18}$$

$$-\left\{\frac{\partial E_z}{\partial n}\right\}_{\Gamma_Q}=\left\{\frac{\partial E_z}{\partial n'}\right\}_B\qquad\text{on}\quad\Gamma_Q. \tag{19}$$

The whole problem addressed can then be finally formulated as in (20), which can be derived easily using (6), (11),

(15), (17), (18), and (19):

$$\begin{bmatrix} \boldsymbol{H}_1 \cdots \boldsymbol{H}_M \ \boldsymbol{H}_Q \ \mathbf{0} \end{bmatrix} \begin{bmatrix} -\boldsymbol{G} \end{bmatrix} \begin{Bmatrix} \{E_z\}_{\Gamma_1} \\ \vdots \\ \{E_z\}_{\Gamma_M} \\ \{E_z\}_{\Gamma_Q} \\ \{E_z\}_{Q} \\ \left\{\frac{\partial E_z}{\partial n'}\right\}_{\Gamma_0} \\ \left\{\frac{\partial E_z}{\partial n'}\right\}_{\Gamma_1} \\ \vdots \\ \left\{\frac{\partial E_z}{\partial n'}\right\}_{\Gamma_M} \\ \left\{\frac{\partial E_z}{\partial n'}\right\}_{\Gamma_Q} \end{Bmatrix} = \begin{Bmatrix} \{0\} \\ \vdots \\ \{0\} \\ \{0\} \\ \{0\} \\ \{0\} \\ 2\delta_{1J}\{f_{11}\} \\ \vdots \\ 2\delta_{MJ}\{f_{M1}\} \\ \{0\} \end{Bmatrix}$$

$$\begin{bmatrix} \mathbf{0} \end{bmatrix} \begin{bmatrix} \boldsymbol{A} \end{bmatrix} \begin{bmatrix} \mathbf{0} & \mathbf{0} \\ \mathbf{0} & \boldsymbol{D} \end{bmatrix}$$

$$\begin{bmatrix} \mathbf{1} \end{bmatrix} \begin{bmatrix} \mathbf{0} \end{bmatrix} \begin{bmatrix} \boldsymbol{Z}_1 & & \mathbf{0} \\ & \ddots & \\ \mathbf{0} & & \boldsymbol{Z}_M \end{bmatrix} \begin{bmatrix} \mathbf{0} \end{bmatrix} \tag{20}$$

In the above equation, [**1**] is an identity matrix, [**0**] is an empty matrix, $\{E_z\}_{\Gamma_i}$ and $\{\partial E_z/\partial n'\}_{\Gamma_i}$ $(i = 0,1,\cdots,M$ and $Q)$ correspond to electric fields and their normal derivatives at the nodal points related to boundary $\Gamma_0, \Gamma_1, \cdots, \Gamma_M, \Gamma_Q$, respectively, and $\{0\}$ is a null vector.

The solution of matrix equation (20) determines the electric field distribution across each waveguide port and, therefore, makes it possible to determine the scattering parameters S_{IJ} of the TE_{10} mode, which are

$$S_{JJ} = \int_0^{W_J} E_z\left(x^{(J)} = 0, y^{(J)}\right) f_{J1}\left(y^{(J)}\right) dy^{(J)} - 1 \tag{21}$$

$$S_{IJ} = \sqrt{\beta_{I1}/\beta_{J1}} \cdot \int_0^{W_I} E_z\left(x^{(I)} = 0, y^{(I)}\right) f_{I1}\left(y^{(I)}\right) dy^{(I)}, \quad i \neq j. \tag{22}$$

These last two equations represent the scattering parameters of the problem shown in Fig. 1 obtained using CFBM, and it will be shown in the next section that this method yields results which are reliable and accurate and at the same time requires much less computer effort than if the FEM were used alone.

III. Numerical Results and Discussion

The coupled finite–boundary element method has been implemented on a VAX-785 computer and many original numerical and experimental results to verify the CFBM have been obtained. The interpolation chosen for the BEM is exactly the same as that for the FEM when field points are located at boundary Γ_Q, which helps to increase the accuracy of the solution. Since no numerical derivatives are needed, accurate results can be obtained without requiring a large number of elements. For all the cases presented below, the power conservation condition has been found to be satisfied to an accuracy of $\pm 10^{-5}$ to 10^{-4}.

As a first example, the Y junction with a TT1-109 triangular ferrite post shown in Fig. 3(a) is considered, where the widths of the three waveguides are the same ($W_1 = W_2 = W_3 = 22.86$ mm). The results obtained with the CFBM solution proposed here and a FEM solution [5] are compared for the parameter values of interest. It is worth mentioning that the CPU time required to solve this problem on a VAX-785 is about 21 minutes and 10 seconds with the FEM alone, while it is about 3 minutes and 35 seconds with the CFBM. Moreover, the CFBM uses only about 13 percent of the memory space required for the FEM. A comparison shows that the results obtained are of the same order of accuracy.

As a second example, the simple configuration of a waveguide corner loaded with a dielectric post shown in Fig. 4 is proposed. In this H-plane corner, the dielectric constant ϵ_r and the width of the square dielectric post a are used as optimization variables to minimize the scattering parameter $|S_{11}|_{\max}$ at eight sampling points uniformly distributed within the whole available band of the waveguide. Curve (*1*) is the optimization result obtained by adjusting ϵ_r and a. Usually, however, ϵ_r is available only in limited values and therefore the optimization is done using the dimension a, which can be easily changed. Curve (*2*) shows the results when ϵ_r is set equal to 2.1 and only the dimension a is used as the optimization variable. Curve (*3*) gives the results with $\epsilon_r = 2.1$ and $\Delta L = 0$, and the numerical results are compared with experimental results represented on the graph by squares. The comparisons in the case without dielectric post shown by curve (*4*), where previous FEM results are shown with dots, are shown to be in good agreement.

Fig. 5 shows the field distribution inside the waveguide corner. It can be seen that the dielectric post plays an important role in concentrating the field, which results in a reduction of the reflections due to the discontinuity.

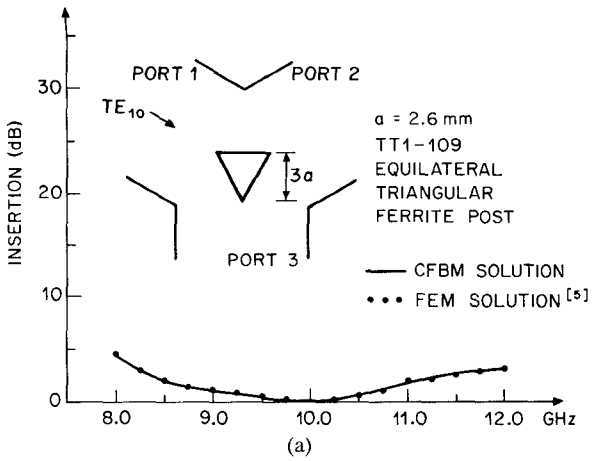

(a)

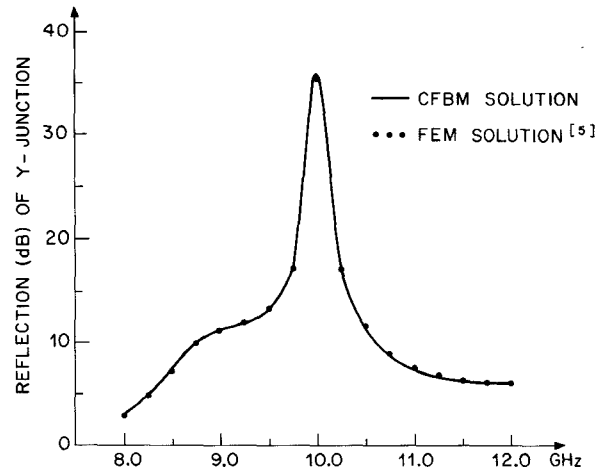

(b)

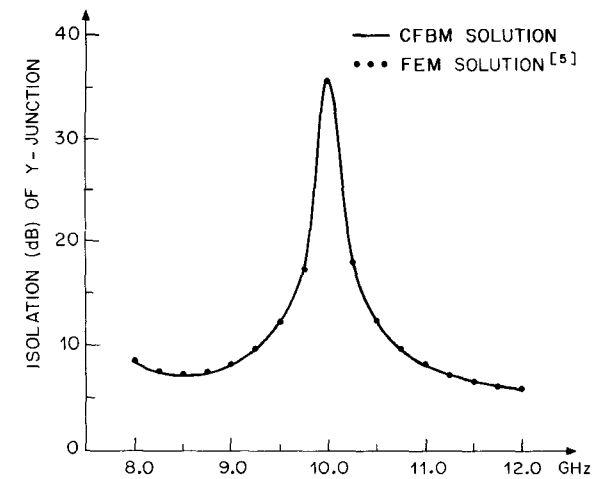

(c)

Fig. 3. Performance of an *X*-band Y junction with a TT1-109 triangular ferrite post and comparison with FEM previous results. (a) Insertion loss. (b) Reflection loss. (c) Isolation loss.

Although only *H*-plane discontinuities have been considered, the extension to the *E*-plane case is rather straightforward. The method can also be easily extended to planar circuits. The problem of analyzing waveguide discontinuties with partial-height posts using the CFBM is presently under consideration.

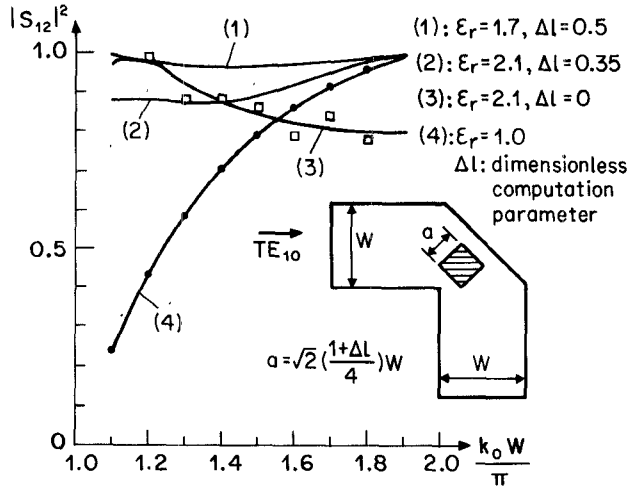

Fig. 4. Power transmission coefficient of a right-angle corner bend in four different cases. Curves (*1*), (*2*), and (*3*) are for three different dielectrics and curve (*4*) corresponds to the case where there is no dielectric.

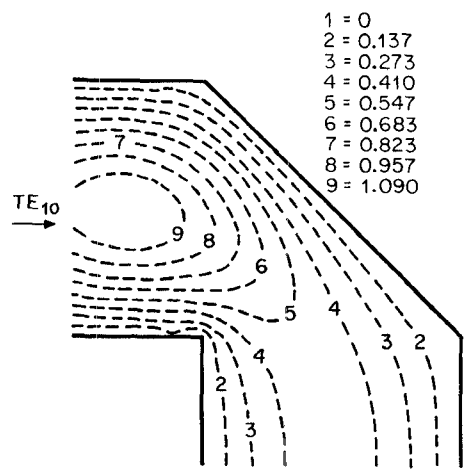

(a)

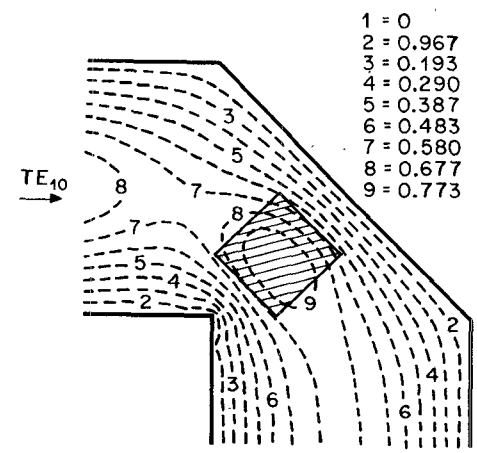

(b)

Fig. 5. Electric field distribution inside the right-angle corner bend of the waveguide: (a) without dielectric load, $k_0W/\pi = 1.2$; (b) with dielectric load, $a = \sqrt{2}/4W$, $k_0W/\pi = 1.2$, $\epsilon_r = 2.1$.

REFERENCES

[1] H. Auda and R. F. Harrington, "Inductive posts and diaphragms of arbitrary shape and number in a rectangular waveguide," *IEEE Trans. Microwave Theory Tech.*, vol. MTT-32, pp. 606–613, June 1984.

[2] Y. Leviatan and G. S. Sheaffer, "Analysis of inductive dielectric posts in rectangular waveguide," *IEEE Trans. Microwave Theory Tech.*, vol. MTT-35, pp. 48–59, Jan. 1987.

[3] A. Wexler, "Solution of waveguide discontinuities by modal analysis," *IEEE Trans. Microwave Theory Tech.*, vol. MTT-15, pp. 509–517, 1967.

[4] J. B. Castillo, Jr., and L. E. Davis, "Computer-aided design of three-port waveguide junction circulators," *IEEE Trans. Microwave Theory Tech.*, vol. MTT-18, pp. 25–34, Jan. 1970.

[5] M. Koshiba and M. Suzuki, "Finite-element analysis of *H*-plane waveguide junction with arbitrarily shaped ferrite post," *IEEE Trans. Microwave Theory Tech.*, vol. MTT-34, pp. 103–109, Jan. 1986.

[6] J. P. Webb and S. Porihar, "Finite element analysis of *H*-plane rectangular waveguide problem," *Proc. Inst. Elec. Eng.*, vol. 133, pt. H, no. 2, pp. 91–94, Apr. 1986.

[7] M. Koshiba, M. Sato, and M. Suzuki, "Application of finite-element method to *H*-plane waveguide discontinuities," *Elecron. Lett.*, vol. 18, pp. 364–365, Apr. 1982.

[8] C. A. Brebbia and S. Walker, *Boundary Element Techniques in Engineering*. London: Newnes-Butterworths, 1980.

[9] S. Kagani and I. Fukai, "Application of boundary-element method to electromagnetic field problems," *IEEE Trans. Microwave Theory Tech.*, vol. MTT-32, pp. 455–461, Apr. 1984.

[10] M. Koshiba and M. Suzuki, "Application of the boundary-element method to waveguide discontinuities," *IEEE Trans. Microwave Theory Tech.*, vol. MTT-34, pp. 301–307, Feb. 1986.

✠

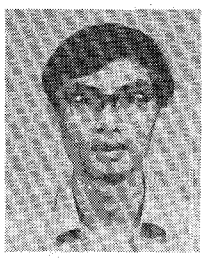

Ke Li Wu was born in Hubei, China, on November 1, 1959. He received the B.S. and M.S.E. degrees in electrical engineering from the East China Institute of Technology, Nanjing, China, in 1982 and 1985, respectively. He is currently a Ph.D. student at Laval University, Quebec, Canada, with research interests in numerical methods for electromagnetic problems, microwave circuits, and microstrip antennas.

✠

Gilles Y. Delisle (S'63–M'73–SM'86) has been a Professor of Electrical Engineering at Laval University, Quebec, Canada, since 1973, where he was head of the department from 1977 to 1983. He is involved in research work in radar cross-section measurements and analytical predictions, mobile radio-channel propagation modeling, and industrial realization of telecommunications equipment.

Dr. Delisle is a senior member of the Order of Engineers of the Province of Quebec, a member of the board of Examiners of this Society, and a member of URSI (Commission B and C) and ACFAS. His work in technology transfer has been recognized by a Canada Award of Excellence in 1986. He has been a consultant in many countries. In 1986 he was awarded the J. Armand Bombardier prize of ACFAS (Association Canadienne Francaise pour l'Avancement des Sciences) for outstanding technical innovation.

✠

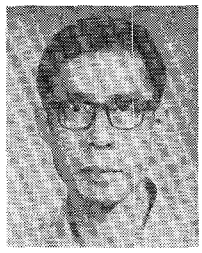

Da Gang Fang was born in Shanghai, China, in 1937 and he received a graduate degree from the Peking Institute of Post and Telecommunication, Department of Radio Engineering, Peking, China, in 1966.

He is presently a Professor at the East China Institute of Technology, Nanjing, China. His research interests are in electromagnetic theory applied to electromagnetic problems, microwave devices and circuits, spectral-domain techniques, microstrip antennas, and millimeter-wave subsystems.

Dr. Fang is the author of two books on antennas and microwave techniques and he was a Visiting Professor at Laval University, Quebec, Canada, in 1980, 1986, and 1988. He is member of the Chinese Institute of Electronics.

✠

Michel Lecours (S'62–M'67–SM'84) graduated from l'Ecole Polytechnique, Montreal, Canada, in 1963, and received the Ph.D. degree in electronics and communication from the Imperial College, London, England, in 1967.

Since 1967, he has been a Professor in the Electrical Engineering Department at Laval University, Quebec, Canada. He was head of the Electrical Engineering Department from 1975 to 1977 and Vice-Dean of the Faculty of Science and Engineering from 1977 to 1985. He has also worked in transmission system engineering at Bell Northern Research in Ottawa and, more recently, as a visiting research scientist in the Digital Mobile Radio Section at the Electrical Communication Laboratories of NTT in Japan.

Dr. Lecours' participation to technology transfer to industry has been recognized by a Canada Award for Excellence in 1986, and in 1987 he was also awarded the Annual Merit Award from the Ecole Polytechnique of Montreal Alumni Association.